

Quantum synchronization

O.V. Zhirov¹ and D.L. Shepelyansky^{2,a}

¹ Budker Institute of Nuclear Physics, 630090 Novosibirsk, Russia

² Laboratoire de Physique Théorique, UMR 5152 du CNRS, Université Paul Sabatier, 31062 Toulouse Cedex 4, France

Received 26 September 2005 / Received in final form 21 November 2005

Published online 17 January 2006 – © EDP Sciences, Società Italiana di Fisica, Springer-Verlag 2006

Abstract. Using the methods of quantum trajectories we study numerically a quantum dissipative system with periodic driving which exhibits synchronization phenomenon in the classical limit. The model allows to analyze the effects of quantum fluctuations on synchronization and establish the regimes where the synchronization is preserved in a quantum case (quantum synchronization). Our results show that at small values of Planck constant \hbar the classical devil's staircase remains robust with respect to quantum fluctuations while at large \hbar values synchronization plateaus are destroyed. Quantum synchronization in our model has close similarities with Shapiro steps in Josephson junctions and it can be also realized in experiments with cold atoms.

PACS. 05.45.Xt Synchronization; coupled oscillators – 03.65.Yz Decoherence; open systems; quantum statistical methods – 74.50.+r Tunneling phenomena; point contacts, weak links, Josephson effects

Since 1665, when Christiaan Huygens discovered the synchronization of two maritime pendulum clocks [1] (see [2,3] for historical survey and modern experiments), it has been established that this universal nonlinear phenomenon appears in an abundant variety of systems ranging from clocks to fireflies, cardiac pacemakers, lasers and Josephson junction (JJ) arrays [3]. Various mathematical tools have been developed to analyze synchronization in simple dissipative nonlinear models with periodic driving and complex ensembles of nonlinear coupled oscillators. Such pure mathematical concepts as Arnold tongues in the circle map [4] found their experimental implementations with Shapiro steps [5] and JJs synchronization [6]. However, till recently the treatment of synchronization has been mainly based on classical mechanics even if JJs have purely quantum origin [3,6].

A significant progress in the theory of dissipative quantum mechanics has been done in reference [7]. It was further developed by various groups as reviewed in [8]. Nowadays this research line is getting more and more importance since technology goes on smaller and smaller scales where an interplay of dissipative and quantum effects becomes dominant. A typical example is given by small size JJs. Here dissipative effects are always present even if in certain cases skillful manipulations allow to realize long term coherent Rabi oscillations [9].

These reasons led to a significant number of analytical studies of quantum tunneling in presence of dissipation (see e.g. [7,8,10–12]). However, analytical methods

have serious restrictions in a strongly nonlinear regime typical of synchronization [3]. Due to that in this paper we perform extensive numerical studies of quantum synchronization following precisely a transition from classical to quantum behavior changing effective dimensionless Planck constant \hbar by three orders of magnitude. The quantum dissipative evolution is described by the master equation for the density matrix ρ written in the Lindblad form [13]. To perform simulations with a large number of states $N \propto 1/\hbar$ we use the method of quantum trajectories [14,15] which allows to reduce significantly the number of equations compared to direct solution of the master equation (N instead of N^2). In this approach one quantum trajectory can be viewed as one individual realization of experimental run [16].

For our studies we choose a model which in the classical limit is closely related to the circle map [4] which gives a generic description of Arnold tongues and synchronization of system dynamics with an external periodic driving [3]. In absence of dissipation the evolution is described by the Hamiltonian of kicked particle falling in a static field f :

$$\hat{H} = \hat{p}^2/2 - f\hat{x} + K \cos \hat{x} \sum_{m=-\infty}^{+\infty} \delta(t - m), \quad (1)$$

with the usual operators \hat{x} and $\hat{p} = \hbar\hat{n} = -i\hbar d/dx$. At $f = 0$ this Hamiltonian corresponds to the kicked rotator [17], a paradigmatic model in the fields of nonlinear dynamics and quantum chaos. At non-zero f the system has been built up in experiments with cold atoms placed in laser fields and falling in a gravitational field

^a <http://www.lpt.irsamc.ups-tlse.fr/~dima/>

[18]. Nontrivial quantum effects of the static force are analyzed in [19]. Here we consider the dynamics of the model in presence of additional friction force $F = -g^2 p$. Experimentally such a force can be realized by the Doppler cooling [20]. The static force f can be also changed continuously creating acceleration in an optical lattice as it has been demonstrated experimentally in [21]. The model can be also implemented with JJs as described in [22]. In this case effective kicks are created by an external *ac*-current source, f and p are proportional respectively to *dc*-current and voltage drop across JJ, while the friction force F naturally appears due to finite circuit resistance. The expression of K and \hbar via JJ parameters is given in [22].

The classical dynamics (1) with friction can be exactly integrated between kicks that gives a dissipative map

$$\begin{aligned} \bar{p} &= (1 - \gamma)p + (1 - \gamma)K \sin x + f\gamma/g^2, \\ \bar{x} &= x + \gamma p/g^2 + (\gamma K/g^2) \sin x + f(g^2 - \gamma)/g^4, \end{aligned} \quad (2)$$

where bars note new values of variables after one map iteration and $1 - \gamma = \exp(-g^2)$. Up to parameter rescaling and shifts in x, p , produced by static force, the map (2) has the form of Zaslavsky map [23]. Due to contraction in p the dynamics in phase variable x is close to the circle map $\bar{x} = x + K_{\text{eff}} \sin x + \nu$ [3,4] and demonstrates devil's staircase structure in the dependence of average momentum P on f (Fig. 1, top). Steps near rational rotation numbers $P/2\pi$ correspond to synchronization with external periodic driving inside Arnold tongues. In average the momentum $P = f/g^2$, as it should be in an equilibrium between the external and friction forces. Inside the horizontal steps in Figure 1 the change of external driving frequency ($\nu \propto f/g^2$) does not change the frequency of the system given by $P/2\pi$. Thus the phase of the system is locked to the phase of external frequency that is called synchronization. The synchronization takes place inside a certain frequency interval near resonant rational values of external frequency where the phase locking is stable. A size of stability region near each resonance grows with the perturbation strength K , such a stability diagram is called Arnold's tongues (see more detailed definitions in Ref. [3]). In analogy with this classical picture we will say that the quantum synchronization takes place when in the quantum system the average frequency $P/2\pi$ shows horizontal steps inside which the system frequency is independent of the external driving frequency. The size of these steps determines the size of quantum Arnold tongues for a given perturbation strength K and \hbar .

The corresponding quantum dissipative dynamics is described by the master equation in the Lindblad form [13]:

$$\dot{\hat{\rho}} = -i[\hat{H}, \hat{\rho}] - \frac{1}{2} \sum_{\mu} \{ \hat{L}_{\mu}^{\dagger} \hat{L}_{\mu}, \hat{\rho} \} + \sum_{\mu} \hat{L}_{\mu} \hat{\rho} \hat{L}_{\mu}^{\dagger}, \quad (3)$$

where $\hat{\rho}$ is the density operator, $\{, \}$ denotes the anticommutator, \hat{L}_{μ} are the Lindblad operators, which model the effects of the environment. Following [24] we assume the

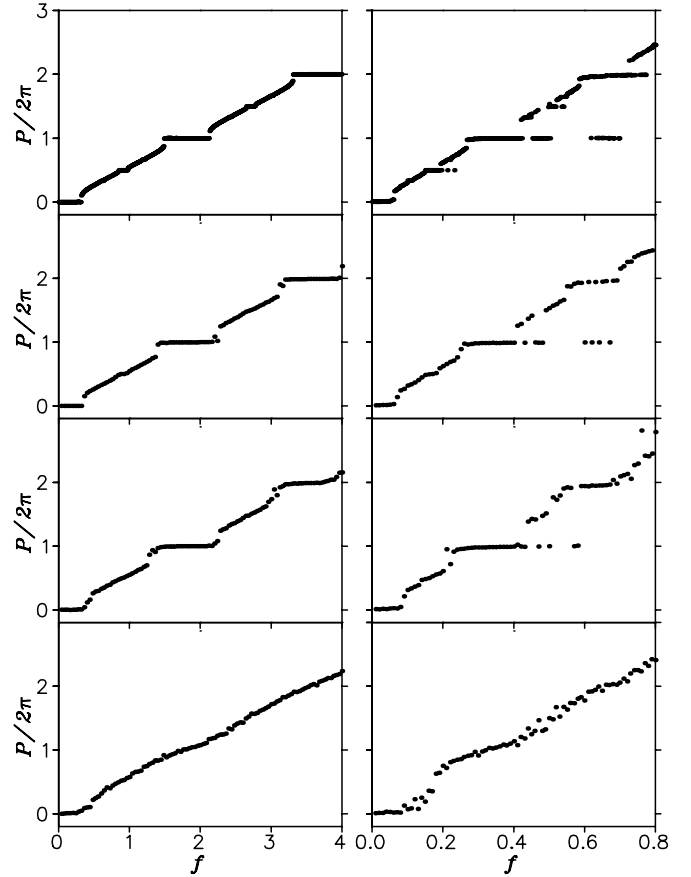


Fig. 1. Dependence of the average momentum P on static force f at $K = 0.8$ for $\gamma = 0.25$ (left column) and $\gamma = 0.05$ (right column); P is computed over $t = 500$ map iterations. From top to bottom: classical case at $\hbar = 0$, $\hbar = 0.12$, $\hbar = 0.05$, $\hbar = 0.5$. Initial conditions correspond to one classical trajectory at $x = 0$, $p/2\pi = 0.38$ for classical dynamics. For the quantum evolution one quantum trajectory is taken at the same x, p position with the wave function in the form of minimal coherent state at given \hbar .

Lindblad operators in the form ($\mu = 1, 2$):

$$\begin{aligned} \hat{L}_1 &= g \sum_n \sqrt{n+1} |n\rangle \langle n+1|, \\ \hat{L}_2 &= g \sum_n \sqrt{n+1} |-n\rangle \langle -n-1|. \end{aligned} \quad (4)$$

These operators act on the bases of 2π -periodic eigenstates of operator \hat{n} and in the regime of weak coupling and Markov approximations describe the dissipation force $F = -g^2 p$ induced by a bosonic bath at zero temperature. As in [24] the numerical simulations of quantum jumps are done for one quantum trajectory using the so-called Monte Carlo wave function approach [16]. The additional term with the constant force f is exactly integrated between jumps leading to a drift of wave function amplitudes in the space of momentum eigenstates n . The total number of states N is fixed by a condition of keeping all states with probabilities higher than 10^{-7} . As in [24], from a wave function $\psi(x)$ of a given quantum trajectory we

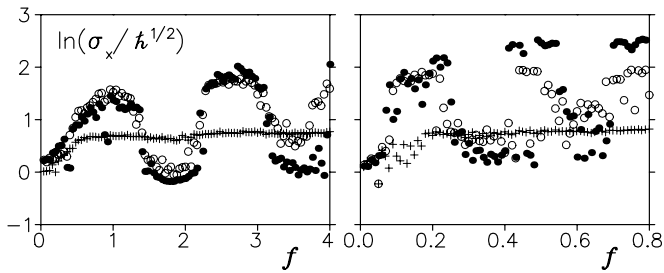


Fig. 2. Dependence of rescaled dispersion $\sigma_x/\hbar^{1/2}$ of wave packet in x on force f for the cases of Figure 1 at $\gamma = 0.25$ (left panel) and $\gamma = 0.05$ (right panel). Symbols show data at $\hbar = 0.012$ (\bullet), $\hbar = 0.05$ (\circ), $\hbar = 0.5$ ($+$). Dispersion σ_x is averaged over $t = 500$ map iterations for one quantum trajectory with initial state of Figure 1.

determine the quantum averaged momentum and position of the wave packet as well as their dispersion values σ_p, σ_x . The momentum P averaged in time is related to the particle displacement by the relation $P = x/t$.

The numerical results for the quantum devil's staircase are shown in Figure 1 for various \hbar values [25]. The dependence is similar to those of $I - V$ characteristics shown in [5] with $P \propto V$, $f \propto I$. At small \hbar values ($\hbar = 0.012$) the steps remains stable with respect to quantum fluctuations. As a result, the rotation frequency is unchanged when f is varied in some finite interval. This can be viewed as the manifestation of quantum synchronization which takes place inside quantum Arnold tongues. For larger $\hbar = 0.05$ small steps start to disappear and at relatively large $\hbar = 0.5$ the dependence $f - P$ becomes smooth so that a quantum particle slides smoothly under static force f . It is interesting to compare the cases of strong $\gamma = 0.25$ and weak $\gamma = 0.05$ dissipation (Fig. 1 left and right columns). At strong γ the contraction in p is rather rapid and the behavior is similar to the case of the circle map [4] and P grows monotonously with f . At weak γ there are many different attractors in the phase space and a classical trajectory may jump between them rather irregularly with variation of f or initial conditions. At small \hbar a quantum trajectory reproduces this behavior of steps overlap rather accurately. We note that very similar structure of steps overlap is clearly seen in experimental data shown in Figure 2 of [5].

To understand the properties of dissipative quantum dynamics we analyze the structure of wave functions associated with quantum trajectories of Figure 1. It is known that dissipation in quantum systems leads to a collapse of wave packet [26–28]. In agreement with these results and recent studies of Zaslavsky map [24] we find that the wave function in our model collapses on a compact packet of width σ_x, σ_p (dispersion) in coordinate and momentum respectively (e.g. $|\psi(x)| \sim \exp(-x^2/(4\sigma_x^2))$) [29]. The width σ_x depends nontrivially on f as it is shown in Figure 2. Inside the steps with synchronization the value of σ_x is strongly reduced while in the sliding regime between steps its value is significantly enhanced. In the limit of small \hbar where quantum synchronization takes place the rescaled width $\sigma_x/\sqrt{\hbar}$ shows approximately the same functional

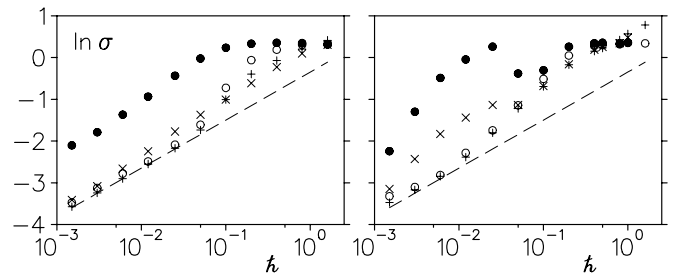


Fig. 3. Dependence of dispersion σ in x (σ_x) and p (σ_p) on \hbar for $K = 0.8$ at $\gamma = 0.25$ (left) and $\gamma = 0.05$ (right); σ is averaged over $t = 5000$ map iterations. Left panel: $f = 1.1$ (\bullet for σ_x and \times for σ_p), $f = 1.9$ (\circ for σ_x and $+$ for σ_p). Right panel: $f = 0.21$ (\bullet for σ_x and \times for σ_p), $f = 0.37$ (\circ for σ_x and $+$ for σ_p). Dashed line shows the dependence $\sigma = (\hbar/2)^{1/2}$. Initial state is as in Figure 1.

dependence on f for all \hbar . This functional dependence on f is completely changed at large \hbar where synchronization is absent and where σ_x is not very sensitive to f . For small γ (Fig. 2 right) the dependence on f becomes more irregular in agreement with more complicated step structure seen in Figure 1 (right). We note that at the same time σ_p remains practically insensitive to variation of f . This is related to the fact that in momentum p the dynamics is close to a simple contraction while in coordinate x the nonlinear dynamics significantly depends on the system parameters (see discussion below).

To check more accurately the scaling $\sigma_x, \sigma_p \propto \sqrt{\hbar}$ we fix two values of force f and vary \hbar by three orders of magnitude (see Fig. 3). One value of f is taken on a synchronization plateau when a classical attractor is a fixed point in the phase space and another is taken on a slope when the classical dynamics has attractor in a form of invariant curve as it is shown in Figure 4 for $\gamma = 0.25$. Clearly σ_x is significantly larger in the case of invariant curve than in the case of fixed point. Intuitively it is rather natural since in the first case variation of phase x is unbounded in 2π while in the later case the phase value is fixed (Fig. 4). Thus we may conclude that quantum synchronization gives a significant reduction of quantum fluctuations. At the same time fluctuations in p characterized by σ_p are not sensitive to the choice of f . In the limit of small \hbar the numerical data of Figure 3 clearly show that the wave packet dispersion scales as

$$\sigma_x \sim \sigma_p \propto \sqrt{\hbar}. \quad (5)$$

In the synchronization regime the dispersion is even close to its minimum value with $\sigma_x \sigma_p = \sigma_p^2 = \hbar/2$ (dashed line in Fig. 3). At smaller dissipation γ the asymptotic dependence $\sigma \propto \sqrt{\hbar}$ starts at smaller values of \hbar (cf. left and right panels of Fig. 3). Indeed, the wave packet width grows dispersively during time $1/\gamma$ that makes σ larger at small γ . The dependence (5) is in agreement with the data obtained in the regime of wave packet collapse in [24] for a smaller range of \hbar variation (note also [29]).

Other properties of quantum dissipative dynamics can be understood from Poincaré phase space plots. In the

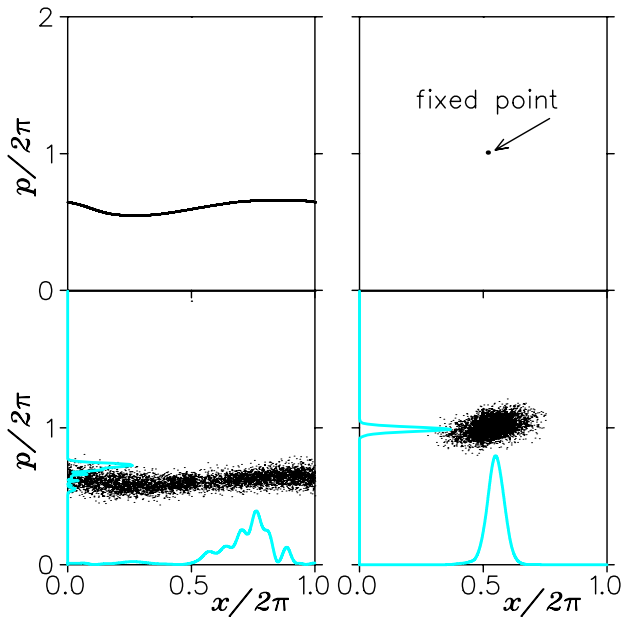


Fig. 4. Poincaré section for $K = 0.8$, $\gamma = 0.25$ at $f = 1.1$ (left) and $f = 1.9$ (right). Top: classical case; bottom: quantum case at $\hbar = 0.05$, points mark the average x, p positions of wave packet; light blue (gray) curves on x, p axes show at $t = 5000$ the quantum probability distribution in x and p respectively (arbitrary units). Number of map iterations $t = 5000$, initial state is as in Figure 1. A colour version of the figure is available in electronic form at <http://www.eurphysj.org>.

classical case two typical examples are shown in Figure 4 (top) with invariant curve and fixed point attractors. In the corresponding quantum case we plot in the phase space the values of x, p averaged over a wave function of a given quantum trajectory at each map iteration (integer time t) (Fig. 4 bottom, quantum probability distributions are also shown). The quantum Poincaré plot reproduces correctly the global structure of classical phase space but additional noise produced by quantum fluctuations is clearly visible. This quantum noise creates an effective width of an invariant curve and replaces a fixed point by a spot of finite size. The size of these fluctuations is approximately given by σ_x and σ_p . They decrease with \hbar according to the relation (5). Due to this quantum noise two quantum trajectories with the same initial state can drop on different attractors and thus contribute to different plateaus in the devil's staircase (Fig. 1). We indeed observed such cases simulating different quantum trajectories with the same initial state. However, convergence to different plateaus takes place only at relatively weak dissipation ($\gamma = 0.05$) when there are many different classical attractors close in a phase space and quantum noise may give transitions between them. At strong dissipation ($\gamma = 0.25$) the attractors are well separated and different quantum trajectories converge to the same plateau.

The above results show that the quantum synchronization has close links with the classical synchronization in presence of noise. The later has been intensively investigated and it is known that the synchronization plateaus

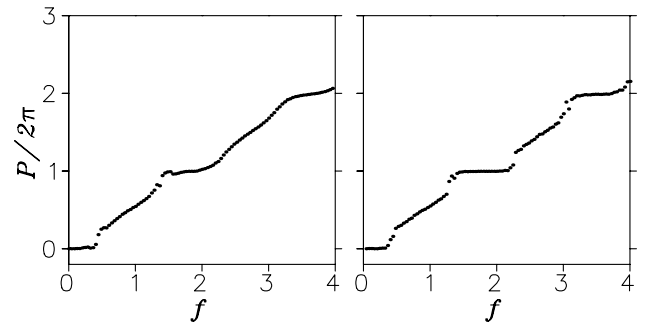


Fig. 5. Dependence of the average momentum P on static force f at $K = 0.8$, $\gamma = 0.25$ (compare with the data in Fig. 1, left column). Right: quantum case at $\hbar = 0.05$ (same data as in Fig. 1, left column). Left: classical simulation of classical dynamics with 200 classical trajectories in presence of noise in x, p with the dispersion of noise corresponding to the values σ_x and σ_p taken from the quantum trajectory simulation at $\hbar = 0.05$ (right).

are preserved if the noise amplitude is significantly smaller than their size [3]. In a similar way we may conclude that the quantum synchronization remains robust with respect to quantum fluctuations until their amplitude (proportional to $\sigma_x, \sigma_p \propto \sqrt{\hbar}$) remains smaller than the size of a synchronization plateau. We also checked that the classical dynamics (2) with additional noise in x, p , with dispersion values σ_x, σ_p taken from the quantum evolution, gives the dependence P vs. f which is close to the quantum result. This is illustrated in Figure 5. This correspondence remains valid if the size of the wave packet is sufficiently small ($\sigma_x, \sigma_p \ll 1$). However, at large \hbar or small γ when $\sigma_x, \sigma_p \sim 1$ this correspondence is broken and the quantum fluctuations cannot be reduced to effects of classical noise.

Above we discussed quantum synchronization with external periodic driving. It would be interesting to investigate the synchronization of two quantum nonlinear pendulum clocks to have a quantum version of the Huygens experiment [1]. Recently, first numerical simulations in such kind of regime (two quantum coupled Duffing oscillators) has been performed in [30]. Their results show that in the case when the quasi-integrable dynamics of oscillators becomes synchronized (entrained) the von Neumann entropy of one oscillator drops significantly. This result is in a qualitative agreement with our data showing that the dispersion of quantum state drops significantly on synchronization plateaus (Fig. 2) [31]. Further investigations of quantum synchronization in coupled nonlinear systems are of great interest. For example, quantization may produce nontrivial effects in the synchronization transition in a disordered JJ series array discussed in [32].

Modern technological progress allows to study the regime of quantum synchronization with small size JJs (e.g. similar to those of [9]) or with cold or BEC atoms (e.g. like in [18]). This should open new perspectives for synchronization of quantum objects with possible applications to quantum computations.

This work was supported in part by the EC IST-FET projects EDIQIP, EuroSQIP and (for OVZ) by RAS Joint scientific program “Nonlinear dynamics and solitons”.

References

1. C. Huygens, *Œuvres complètes* (Swets & Zeitlinger B.V., Amsterdam, 1967), Vol. 15
2. M. Bennett, M.F. Schatz, H. Rockwood, K. Wiesenfeld, Proc. R. Soc. Lond. A **458**, 563 (2002)
3. A. Pikovsky, M. Rosenblum, J. Kurths, *Synchronization: a universal concept in nonlinear sciences* (Cambridge University Press, Cambridge UK, 2001)
4. V.I. Arnold, Izv. Akad. Nauk SSSR Ser. Mat. **25**, 21 (1961) [AMS Transl. Ser. 2, **28**, 61 (1963)]
5. S. Shapiro, Phys. Rev. Lett. **11**, 80 (1963)
6. A.K. Jain, K.K. Likharev, J.E. Lukens, J.E. Sauvageau, Phys. Rep. **109**, 309 (1984)
7. A.O. Caldeira, A.J. Leggett, Phys. Rev. Lett. **46**, 211 (1981); A.D. Caldeira, A.J. Leggett, Ann. Phys. (N.Y.) **149**, 374 (1983)
8. U. Weiss, *Quantum dissipative systems* (World Sci., Singapore, 1999)
9. D. Vion, A. Aassime, A. Cottet, P. Joyez, H. Pothier, C. Urbina, D. Esteve, M.H. Devoret, Science **296**, 886 (2002)
10. A.J. Leggett, S. Chakravarty, A.T. Dorsey, M.P.A. Fischer, A. Garg, W. Zwerger, Rev. Mod. Phys. **59**, 1 (1987)
11. Y.N. Ovchinnikov, B.I. Ivlev, Phys. Rev. B **39**, 9000 (1989)
12. D.V. Averin, A.A. Odintsov, Sov. J. Low Temp. Phys. **16**, 7 (1990); D.V. Averin, A.A. Odintsov, Sov. J. Low Temp. Phys. **16**, 725 (1990)
13. G. Lindblad, Commun. Math. Phys. **48**, 119 (1976)
14. T.A. Brun, I.C. Percival, R. Schack, J. Phys. A **29**, 2077 (1996)
15. T.A. Brun, Am. J. Phys. **70**, 719 (2002)
16. J. Dalibard, Y. Castin, K. Mølmer, Phys. Rev. Lett. **68**, 580 (1992)
17. F.M. Izrailev, Phys. Rep. **196**, 299 (1990)
18. Z.-Y. Ma, M.B. d’Arcy, S.A. Gardiner, Phys. Rev. Lett. **93**, 164101 (2004)
19. S. Wimberger, I. Guarneri, S. Fishman, Phys. Rev. Lett. **92**, 084102 (2004)
20. M.O. Scully, M.S. Zubairy, *Quantum Optics* (Cambridge University Press, Cambridge, UK, 1997)
21. S.R. Wilkinson, C.F. Bharucha, K.W. Madison, Q. Niu, M.G. Raizen, Phys. Rev. Lett. **76**, 4512 (1996)
22. R. Graham, M. Schlautmann, D.L. Shepelyansky, Phys. Rev. Lett. **67**, 255 (1991)
23. G.M. Zaslavsky, Phys. Lett. A **69**, 145 (1978)
24. G. Carlo, G. Benenti, D.L. Shepelyansky, Phys. Rev. Lett. **95**, 164101 (2005)
25. We show here data for one typical case at $K = 0.8$, similar results have been seen in the range $0.4 \leq K \leq 2$ with quasi-integrable dynamics
26. I.C. Percival, J. Phys. A **27**, 1003 (1994)
27. J. Halliwell, A. Zoupas, Phys. Rev. D **52**, 7294 (1995)
28. R. Schack, T.A. Brun, I.C. Percival, J. Phys. A **28**, 5401 (1995)
29. We study here the nonlinear dynamics in a quasi-integrable regime without Ehrenfest explosion [24]
30. M.J. Everitt, T.D. Clark, P.B. Stiffell, J.F. Ralph, A.R. Bulsara, C.J. Harland, New J. Phys. **7**, 64 (2005)
31. Let us note that a large value of entropy found in [30] in the chaotic regime at small \hbar should be related to the Ehrenfest explosion discussed in [24]
32. K. Wiesenfeld, P. Colet, S.H. Strogatz, Phys. Rev. Lett. **76**, 404 (1996)